

# NONSTATIONARY ARRAY PROCESSING FOR TRACKING MOVING TARGETS WITH TIME-VARYING POLARIZATIONS

Baha A. Obeidat, Yimin Zhang, and Moeness G. Amin

Center for Advanced Communications  
 Villanova University, Villanova, PA 19085, USA  
 E-mail: {baha.obeidat,yimin.zhang,moeness.amin}@villanova.edu

## ABSTRACT

*This paper presents an approach for tracking nonstationary moving sources with both time-varying directions-of-arrival (DOAs) and time-varying polarization signatures. The proposed approach is based on the spatial polarimetric time-frequency distributions (SPTFDs). Unlike the conventional correlation matrix based approaches that sacrifice the source signal polarization properties and are not properly structured to utilize polarization diversity, the proposed approach uses the signal instantaneous polarization and instantaneous frequency information for improved target tracking and polarization estimation.*

## 1. INTRODUCTION

Signals of time-varying spectral characteristics are employed in various radar systems due to their attractive properties [1][2]. Waveform polarization is another attractive property which has received much interest in radar systems (polarimetric SAR [3]) and multisensor technologies [4]. The spatial polarimetric time-frequency distributions (SPTFDs) have been introduced in [5, 6] as a platform to process nonstationary polarimetric signals incident on multi-sensor receivers.

Commonly, radar signal returns have polarization properties that are time-varying in nature [7]. The polarization signature can be utilized in the identification of target (e.g., human, aircraft), clutter, or terrain. Multisensor systems that use a single- or double-feed dual-polarized array of sensors outperform their non-polarimetric counterparts in estimating the target DOA. However, when dealing with time-varying polarization sources, conventional covariance matrix based approaches are not structured to fully utilize the sources' polarization characteristics. These approaches can only capture the instantaneous polarization with the application of a short observation time window that renders it inadequate in low SNRs.

This paper introduces an approach for tracking moving targets whose DOAs and polarization signatures are both time-varying. The spatial polarimetric time-frequency distributions (SPTFDs) are used for the purpose of localiz-

ing the signal energy in the time-frequency domain. The proposed approach exploits the instantaneous polarization diversity among the source signals which provides an additional degree of freedom, leading to improved signal and noise subspace estimates for DOA estimations.

## 2. SIGNAL MODEL

Consider an array of  $M$  dual-polarized sensors, where the vertically polarized sensors are placed along the  $z$ -axis and the horizontally polarized sensors are placed along the  $y$ -axis (Fig. 1). For simplicity, it is assumed that the source signals are located in the  $x$ - $y$  plane and they impinge upon the array with time-varying DOAs of  $\phi_n(t)$ ,  $n = 1, \dots, N$ .

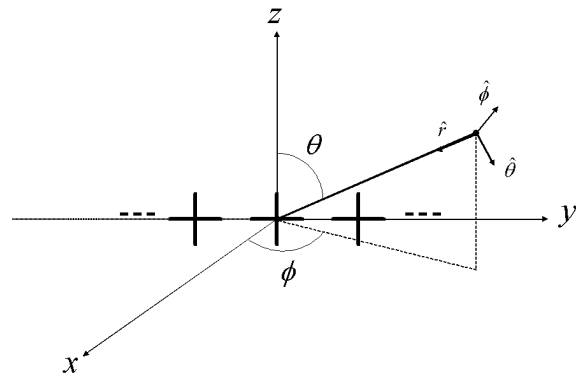


Figure 1: Dual-polarized array.

The  $N$  source signals are modelled as transverse electromagnetic (TEM) waves with time-varying DOAs and polarizations. The EM field is described generally as

$$\vec{\mathbf{E}}(t) = \sum_{n=1}^N s_n(t) [-\cos(\gamma_n(t)) \sin(\phi_n(t)) \hat{x} + \cos(\phi_n(t)) \sin(\gamma_n(t)) e^{j\eta_n(t)} \hat{y} + \cos(\gamma_n(t)) \hat{z}], \quad (1)$$

where the polarization angle,  $\gamma_n(t)$ , and phase difference,  $\eta_n(t)$ , together describe the signals' time-varying polarization, with  $n = 1, \dots, N$ . It is worth noting that the  $x$ -axis component is not received by the dual-polarized antennas,

This work was supported in part by the ONR under Grant No. N00014-98-1-0176 and DARPA under Grant No. MDA972-02-1-0022. The content of the information does not necessarily reflect the position or the policy of the Government, and no official endorsement should be inferred.

whereas the  $\cos(\phi_n(t))$  term along the  $y$ -axis can be absorbed in the array calibration. The received signal at the  $m$ th vertical sensor is given by

$$x_m^{[v]}(t) = \sum_{n=1}^N a_{mn}^{[v]}(t) \cos(\gamma_n(t)) s_n(t), \quad (2)$$

whereas the signal at the  $m$ th horizontal sensor is

$$x_m^{[h]}(t) = \sum_{n=1}^N a_{mn}^{[h]}(t) \sin(\gamma_n(t)) e^{j\eta_n(t)} s_n(t) \quad (3)$$

where  $a_{mn}^{[v]}(t)$  and  $a_{mn}^{[h]}(t)$ , respectively, represent the time-varying propagation phase delay for the two signal polarization components. They are the  $m$ th elements of their respective array response vectors,  $\mathbf{a}^{[v]}(\phi_n(t))$  and  $\mathbf{a}^{[h]}(\phi_n(t))$ , for the two polarizations.

In vector form, the received signals in both polarizations are concatenated resulting in an dimension-extended received signal vector

$$\mathbf{x}(t) = \begin{bmatrix} \mathbf{A}^{[v]}(\Phi(t))(\mathbf{q}^{[v]}(t) \odot \mathbf{s}(t)) \\ \mathbf{A}^{[h]}(\Phi(t))(\mathbf{q}^{[h]}(t) \odot \mathbf{s}(t)) \end{bmatrix} + \begin{bmatrix} \mathbf{n}^{[v]}(t) \\ \mathbf{n}^{[h]}(t) \end{bmatrix} \quad (4)$$

where  $\odot$  denotes the Hadamard product operator,  $\mathbf{A}^{[i]}(\Phi(t)) = [\mathbf{a}^{[i]}(\phi_1(t)) \ \dots \ \mathbf{a}^{[i]}(\phi_N(t))]$ ,  $i = v, h$ , are the array response matrices, and  $\mathbf{s}(t) = [s_1(t) \ \dots \ s_N(t)]^T$  is the source signal vector. In addition, the  $M \times 1$  size vectors,  $\mathbf{n}^{[v]}(t)$  and  $\mathbf{n}^{[h]}(t)$ , are the additive sensor noise and are assumed to be zero-mean and spatially and temporally white. The  $N$ -dimensional vector  $\Phi(t) = [\phi_1(t) \ \dots \ \phi_N(t)]$  represents the time-varying DOAs of the  $N$  sources. A total of  $T$  samples ( $1 \leq t \leq T$ ) are considered. The two time-dependent polarization vectors which contain information of the  $N$  source signals in the vertical and horizontal polarizations are, respectively,

$$\begin{aligned} \mathbf{q}^{[v]}(t) &= [\cos(\gamma_1(t)), \dots, \cos(\gamma_N(t))]^T, \\ \mathbf{q}^{[h]}(t) &= [\sin(\gamma_1(t))e^{j\phi_1(t)}, \dots, \sin(\gamma_N(t))e^{j\phi_N(t)}]^T. \end{aligned} \quad (5)$$

### 3. MOVING SOURCES WITH TIME-VARYING POLARIZATIONS

Consider the pseudo Wigner-Ville distribution (PWVD) as the example in implementing the SPTFD. The discrete form of the spatial polarimetric pseudo Wigner-Ville distribution (SPPWVD) is given by [8]

$$\mathbf{D}_{\mathbf{xx}}(t, f) = \sum_{\tau=-(L-1)/2}^{(L-1)/2} \mathbf{x}(t+\tau)\mathbf{x}^H(t-\tau)e^{-j4\pi f\tau}, \quad (6)$$

where  $L$  is odd and defines the window length, and  $H$  denotes the Hermitian transpose. Substituting (4) in (6) yields a  $2M \times 2M$  spatial time-frequency distribution matrix with expected value

$$E[\mathbf{D}_{\mathbf{xx}}(t, f)] = \begin{bmatrix} E[\mathbf{D}_{\mathbf{x}^{[v]}\mathbf{x}^{[v]}}(t, f)] & E[\mathbf{D}_{\mathbf{x}^{[v]}\mathbf{x}^{[h]}}(t, f)] \\ E[\mathbf{D}_{\mathbf{x}^{[h]}\mathbf{x}^{[v]}}(t, f)] & E[\mathbf{D}_{\mathbf{x}^{[h]}\mathbf{x}^{[h]}}(t, f)] \end{bmatrix} + \sigma^2 \mathbf{I}_{2M}, \quad (7)$$

where  $\sigma^2$  denotes the noise power at each single-polarized antenna and  $\mathbf{I}_{2M}$  is the  $2M \times 2M$  identity matrix. Moreover,  $\mathbf{D}_{\mathbf{x}^{[i]}\mathbf{x}^{[k]}}(t, f)$ ,  $i, k = v, h$ , is the auto- ( $i = k$ ) or cross-polarized ( $i \neq k$ ) SPPWVD matrix. Ignoring the noise, each element of the  $2M \times 2M$  block matrix in (7) can be expressed as

$$\begin{aligned} & \mathbf{D}_{\mathbf{x}^{[i]}\mathbf{x}^{[k]}}(t, f) \\ &= \sum_{\tau=-(L-1)/2}^{(L-1)/2} \mathbf{A}^{[v]}(\Phi(t+\tau)) \left[ \mathbf{q}^{[i]}(t+\tau)(\mathbf{q}^{[k]}(t-\tau))^H \right] \\ & \quad \odot \left[ \mathbf{s}(t+\tau)\mathbf{s}^H(t-\tau) \right] \left[ \mathbf{A}^{[v]}(\Phi(t-\tau)) \right]^H e^{-j4\pi f\tau} \\ &= \sum_{\tau=-(L-1)/2}^{(L-1)/2} \mathbf{A}^{[v]}(\Phi(t+\tau)) \left[ \mathbf{G}^{[ik]}(t, \tau) \odot \mathbf{K}(t, \tau) \right] \\ & \quad \left[ \mathbf{A}^{[v]}(\Phi(t-\tau)) \right]^H e^{-j4\pi f\tau} \end{aligned} \quad (8)$$

with  $\mathbf{G}^{[ik]}(t, \tau) = \mathbf{q}^{[i]}(t+\tau)(\mathbf{q}^{[k]}(t-\tau))^H$  and  $\mathbf{K}(t, \tau) = \mathbf{s}(t+\tau)\mathbf{s}^H(t-\tau)$ . For a small value of  $L$ , Eq. (8) can be approximated by [8]

$$\mathbf{D}_{\mathbf{x}^{[i]}\mathbf{x}^{[k]}}(t, f) \simeq \mathbf{A}^{[v]}(\Phi(t))\mathbf{D}_{\mathbf{s}^{[i]}\mathbf{s}^{[k]}}(t, f) \left[ \mathbf{A}^{[v]}(\Phi(t)) \right]^H \quad (9)$$

where

$$\mathbf{D}_{\mathbf{s}^{[i]}\mathbf{s}^{[k]}}(t, f) = \sum_{\tau=-(L-1)/2}^{(L-1)/2} \mathbf{G}^{[ik]}(t, \tau) \odot \mathbf{K}(t, \tau) e^{-j4\pi f\tau}. \quad (10)$$

We assume that the frequency and the polarization signatures of the sources change almost linearly over the window length. Accordingly, using the first-order Taylor-series expansion, the polarization-dependent terms can be approximated as  $\gamma_n(t+\tau) = \gamma_n(t) + \tau\dot{\gamma}_n(t)$ , where  $\dot{\gamma}_n(t) = \frac{d}{dt}\gamma_n(t)$ . The autoterms of the source polarization information, which reside on the diagonals of  $\mathbf{G}^{[vv]}(t, \tau)$ ,  $\mathbf{G}^{[vh]}(t, \tau)$ ,  $\mathbf{G}^{[hv]}(t, \tau)$  and  $\mathbf{G}^{[hh]}(t, \tau)$ , are given by

$$\left[ \mathbf{G}^{[vv]}(t, \tau) \right]_{nn} = \frac{1}{2} [\cos(2\gamma_n(t)) + \cos(2\tau\dot{\gamma}_n(t))] \quad (11)$$

$$\left[ \mathbf{G}^{[vh]}(t, \tau) \right]_{nn} = \frac{1}{2} [\sin(2\gamma_n(t)) - \sin(2\tau\dot{\gamma}_n(t))] \quad (12)$$

$$\left[ \mathbf{G}^{[hv]}(t, \tau) \right]_{nn} = \frac{1}{2} [\sin(2\gamma_n(t)) + \sin(2\tau\dot{\gamma}_n(t))] \quad (13)$$

$$\left[ \mathbf{G}^{[hh]}(t, \tau) \right]_{nn} = \frac{1}{2} [-\cos(2\gamma_n(t)) + \cos(2\tau\dot{\gamma}_n(t))], \quad (14)$$

respectively. Due to symmetry, the contributions of the second sinusoidal terms in Eqs. (12) and (13) to  $\mathbf{D}_{\mathbf{s}^{[i]}\mathbf{s}^{[k]}}(t, f)$  cancel out. Therefore, the diagonal elements of  $\mathbf{D}_{\mathbf{s}^{[i]}\mathbf{s}^{[k]}}(t, f)$  (or the autoterm points) can be expressed as

$$D_{s_n^{[v]}s_n^{[v]}}(t, f) = \frac{1}{2} \cos(2\gamma_n(t))D_{s_n s_n}(t, f) + c_{nn}(t, f) \quad (15)$$

$$D_{s_n^{[h]}s_n^{[h]}}(t, f) = -\frac{1}{2} \cos(2\gamma_n(t))D_{s_n s_n}(t, f) + c_{nn}(t, f) \quad (16)$$

$$D_{s_n^{[v]}s_n^{[h]}}(t, f) = D_{s_n^{[h]}s_n^{[v]}}(t, f) = \frac{1}{2} \sin(2\gamma_n(t))D_{s_n s_n}(t, f), \quad (17)$$

where

$$c_{nn}(t, f) = \frac{1}{2} \sum_{\tau=-(L-1)/2}^{(L-1)/2} \cos(2\tau\dot{\gamma}_n(t)) [\mathbf{K}(t, \tau)]_{nn} e^{-j4\pi f\tau}. \quad (18)$$

If the time-frequency (t-f) points located in the autoterm region of the  $n$ th source are used in constructing the SPTFD matrix, then

$$\mathbf{D}_{\mathbf{x}\mathbf{x}}(t, f) = \mathbf{A}(\phi_n(t))\mathbf{M}\mathbf{A}^H(\phi_n(t)) \quad (19)$$

where

$$\mathbf{A}(\phi_n(t)) = \begin{bmatrix} \mathbf{a}^{[v]}(\phi_n, t) & 0 \\ 0 & \mathbf{a}^{[h]}(\phi_n, t) \end{bmatrix} \quad (20)$$

$$\mathbf{M} = \frac{1}{2} D_{s_n s_n}(t, f) \begin{bmatrix} \cos(2\gamma_n(t)) & \sin(2\gamma_n(t)) \\ \sin(2\gamma_n(t)) & -\cos(2\gamma_n(t)) \end{bmatrix} + \begin{bmatrix} c_{nn}(t, f) & 0 \\ 0 & c_{nn}(t, f) \end{bmatrix}. \quad (21)$$

In the new structure of the SPTFD matrix of Eq. (19), the time-varying source polarization has the effect of loading the diagonal elements with  $c_{nn}(t, f)$  and, as such, alters the eigenvalues of the above  $2 \times 2$  matrix. However, the eigenvectors of  $\mathbf{M}$  remain unchanged. The new eigenvalues are  $\lambda_{1,2} = c(t, f) \pm \frac{1}{2} D_{ss}(t, f)$ . The signal polarization signature, i.e., the eigenvector corresponding to the maximum eigenvalue at the particular time point in (21), is  $\mathbf{v}_1 = [\cos(\gamma_n(t)) \quad \sin(\gamma_n(t))]^T$ . Therefore, in the context of polarization-based subspace-based estimation, such as the PTF-MUSIC [6] or PTF-ESPRIT [9], the instantaneous polarization characteristics can be utilized for source discriminations, instantaneous DOA estimation, and target tracking.

It is noted that, while the above analysis is applied to a t-f point pertaining to one source only, the extension of the above observations to the situation where the t-f point is common to more than one source or when multiple t-f points are used for SPTFD matrix construction is straightforward. In both cases, t-f points should be selected over time periods during which there are differences in the source local polarizations.

#### 4. SIMULATIONS

Figure 2 shows the polarization-averaged pseudo Wigner-Ville distribution (PWVD) of the received data at the reference sensor with a window length of 63. The two chirp signals present have the parameters listed in Table 1. The two sources impinge on a uniform linear array (ULA) of five cross-dipoles with an interelement spacing of half a wavelength. The array responses in both horizontal and vertical polarizations are identical. The SNR is 10dB. The source signals' polarization angles ( $\gamma_n, n = 1, 2$ ) change linearly with time over the observation period of  $T = 256$  samples and are shown in Fig. 3. In addition, the source signals' DOAs change linearly over the same period, as shown in Fig. 4. In tracking the moving sources' DOAs, different sets of SPTFD matrices are constructed, where each set uses  $P$  consecutive (neighboring) t-f points of the two sources'

autoterms, with the middle t-f point being at  $t_i$ . The objective is to examine the proposed algorithm performance at different source polarization states and to demonstrate the tracking accuracy of the algorithm. This is achieved by applying the PTF-MUSIC for each set of SPTFD matrices separately.

Table 1: Signal Parameters

	start freq.	end freq.	DOA (deg)	$\gamma$ (deg)	$\eta$ (deg)
source 1	0.00	0.40	-20 to 0	0 to 90	0
source 2	0.30	0.70	0 to 20	90 to 0	0

Figure 5(a) shows the root mean square error (RMSE) performance over 200 trials of the PTF-MUSIC algorithm for the estimation of the DOA of the first source with  $P = 31$  and using a PWVD with window length  $L = 63$ . Fig. 5(b) shows the RMSE performance where only the time-frequency points in the autoterm region of source 1 are used for the PTF-MUSIC. The performance of the covariance matrix-based polarimetric MUSIC (P-MUSIC) is also shown in both figures for  $P = 95$ . The RMSE was generated at 49 time points that are spaced 5 samples apart (i.e.,  $t_1 = 8$  and  $t_{49} = 248$ ). We note that both techniques use the same data samples for each RMSE. Fig. 6 shows a tracking trial for the two algorithms. The PTF-MUSIC generally outperforms the P-MUSIC as can be seen in Figs. 5 and 6. The performance of the PTF-MUSIC is particularly impressive in the middle region where the source polarization discrimination is affected due to the similarity in the source signals' polarization characteristics. However, at the edge points the PTF-MUSIC experiences performance degradation due to the use of a windowed PWVD and the subsequent spreading of the source signals' energy in the PWVD as can be seen in Fig. 2.

#### 5. CONCLUSIONS

We have presented an enhanced approach for estimating the signal polarization and tracking nonstationary moving sources incident on a double-feed dual-polarized sensor array. The spatial polarimetric time-frequency distributions (SPTFDs) uses the source power localization property and utilizes the distinctions in the time-varying frequency and polarization signatures of the different sources in the field of view, leading to improved direction-of-arrival (DOA) tracking and polarization state estimation performance.

#### REFERENCES

- [1] S. Qian and V. Chen, *Joint Time-Frequency Analysis — Methods and Applications*, Englewood Cliffs, NJ: Prentice Hall, 1996.
- [2] A. B. Gershman, M. Pesavento, and M. G. Amin, "Estimating parameters of multiple wideband polynomial-phase source in sensor arrays," *IEEE Trans. Signal Processing*, vol. 49, no. 12, pp. 2924–2934, Dec. 2001.
- [3] W.M. Boerner, "Recent advances in extra-wide-band polarimetry, interferometry and polarimetric interferometry in synthetic aperture remote sensing and its applications," *IEE Proceedings - Radar, Sonar and Navigation*, vol. 150, no. 3, pp. 113–124, June 2003.

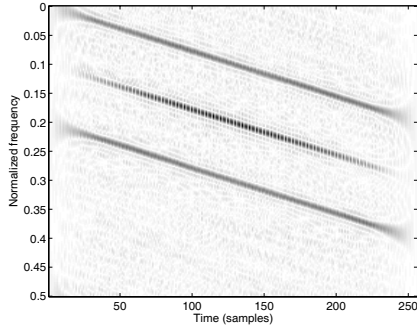


Figure 2: Polarization-averaged PWVD of the received data at the reference sensor.

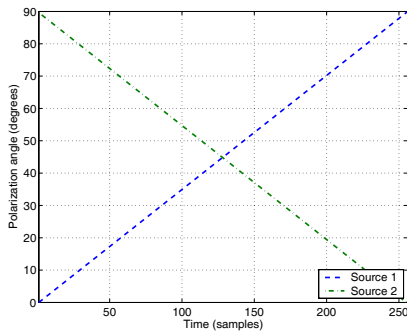


Figure 3: Source time-varying polarization signatures.

- [4] R. U. Nabar, H. Bolcskei, V. Erceg, D. Gesbert, and A. J. Paulraj, "Performance of multiantenna signaling techniques in the presence of polarization diversity," *IEEE Trans. Signal Processing*, vol. 50, no. 10, pp. 2553–2562, Oct. 2002.
- [5] Y. Zhang, M. G. Amin, and B. A. Obeidat, "The spatial polarimetric time-frequency distributions and their application to direction-of-arrival estimation," *Proc. SPIE*, vol. 5205, pp. 75–85, Aug. 2003.
- [6] Y. Zhang, B. A. Obeidat, and M. G. Amin, "Spatial polarimetric time-frequency distributions for direction-of-arrival estimations," *IEEE Trans. Signal Processing*, submitted.
- [7] V. Santalla and Y. M. M. Antar, "A comparison between different polarimetric measurement schemes," *IEEE Trans. Geoscience and Remote Sensing*, vol. 40, no. 5, pp. 1007–1017, May 2002.
- [8] A. B. Gershman and M. G. Amin, "Wideband direction-of-arrival estimation of multiple chirp signals using spatial time-frequency distributions," *IEEE Signal Processing Letters*, vol. 7, no. 6, pp. 152–155, June 2000.
- [9] B. A. Obeidat, Y. Zhang, and M. G. Amin, "Polarimetric time-frequency ESPRIT," *Asilomar Conf. Signals, Sys., and Comput.*, Pacific Grove, CA, Nov. 2003.
- [10] R. O. Schmidt, "Multiple emitter location and signal parameter estimation," *IEEE Trans. Antennas Propagat.*, vol. 34, no. 3, pp. 276–280, March 1986.

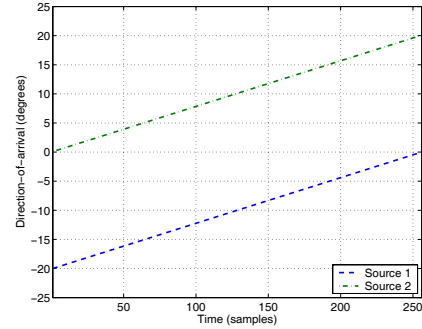
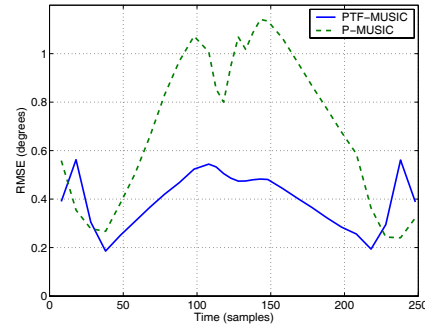
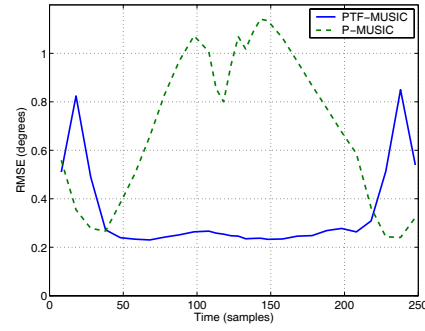


Figure 4: Source time-varying angle signatures.



(a) Performance comparison



(b) Performance with PTF-MUSIC applying source discrimination

Figure 5: P-MUSIC and PTF-MUSIC tracking of source 1.

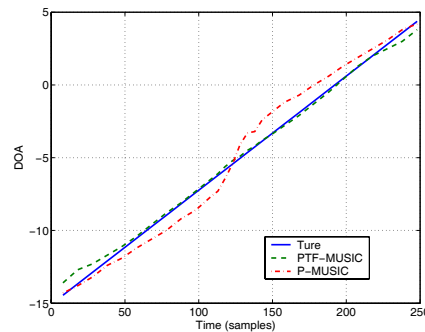


Figure 6: Single trial P-MUSIC and PTF-MUSIC tracking for source 1.